

Adsorption and Corrosion Inhibition Behavior of C38 Steel by one Derivative of Quinoxaline in 1 M HCl

M. Elayyachy, B. Hammouti,* A. El Idrissi and A. Aouniti

LCAE-URAC18, Faculté des Sciences, Université Mohammed Premier,
B.P. 717, 60000 Oujda, Morocco

Received 15 November 2010; accepted 28 February 2011

Abstract

The influence of 2-[3-(2-oxo-2-phenylethylidene)-1,4-dihydroquinoxaline-2(1H)-ylidene]-1-phenylethanone (Qx1) and amino-2-aniline (Diam1) on the corrosion of steel in 1 M HCl solution has been investigated by weight loss measurements, potentiodynamic polarisation and impedance spectroscopy (EIS) methods. The inhibiting action increases with the concentration of Qx1 and Diam1. The highest efficiency (85%) is obtained at the 10^{-4} M Qx1. There is good agreement between gravimetric and electrochemical methods (potentiodynamic polarisation and EIS). Polarisation measurements also show that Qx1 and Diam1 act as mixed inhibitors. The cathodic curves indicate that the reduction of proton at the steel surface happens with an activating mechanism. Qx1 adsorbs on the steel surface according to Langmuir adsorption model. Effect of temperature is also studied between 308 and 353 K.

Keywords: quinoxaline, inhibition, corrosion, steel, acid.

Introduction

Addition of inhibitor remains the necessary procedure to secure the metal against acid attack in chemical cleaning and pickling to remove mill scales (oxide scales) from the metallic surface. Inhibitors should be effective even under severe conditions in concentrated hydrochloric acid (20%) at temperatures up to 60 °C. Organic compounds rich in heteroatoms such as sulphur, nitrogen and oxygen generally exhibit the best protection for corrosion. Among these inhibitors, diamines [1-4] are efficient ones in corrosive media. Their adsorption is generally explained by the formation of an adsorptive film of a physical and/or chemical character on the metal surface. The synthesis of new organic molecules

* Corresponding author. E-mail address: hammoutib@gmail.com

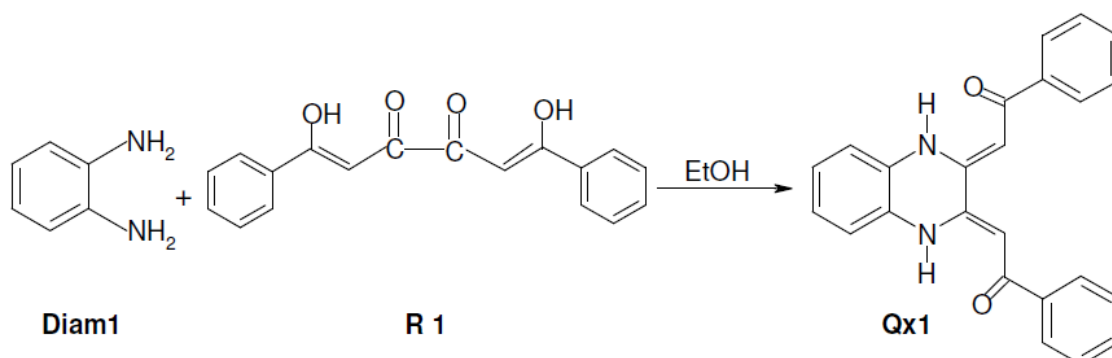
offers various molecular structures containing several heteroatoms and substituents. Our research in these latest decennia has permitted us to classify several series such of compounds namely aminoacid and aminoester [5-11], pyrazole [12-18], and pyridine [19-23] as effective corrosion inhibitors. The continuation of our work on development of organic compounds as acid inhibitors is oriented to a new series of quinoxaline compounds. The good inhibitory effect of quinoxaline derivatives [24-27] has incited us to test another quinoxaline derivative: 2-[3-(2-oxo-2-phenylethylidene)-1,4-dihydroquinoxaline-2(1H)-ylidene]-1-phenyl ethanone (Qx1) as corrosion inhibitor for steel in 1 M HCl in the 308-353 K range. The quinoxaline ring is part of many polycyclic compounds of biological or industrial significance. The anti-tuberculosic, anti-cancer activities, anti-mycobacterial, anti-trichomonas and anti-candida data of quinoxaline derivatives have been reported [28-31].

The objective of the present work therefore is to study the mechanism of corrosion inhibition of the newly synthesized quinoxaline derivative and its reactant diamine on steel surface (Scheme 1). The behaviour of 2-[3-(2-oxo-2-phenylethylidene)-1,4-dihydroquinoxaline-2(1H)-ylidene]-1-phenylethanone (Qx1) and amino-2-aniline (Diam1) as a corrosion inhibitor for metals is reported using the weight loss method, potentiodynamic polarization and electrochemical impedance spectroscopy (EIS).

Experimental

Inhibitors

The quinoxaline compound (Qx1) was synthesised from amino-2-aniline (Diam1) and 1,6-dihydroxy-1,6-diphenylhexa-1,5-diene-3,4-dione (R1), according to scheme 1. It was purified and characterised by N.M.R. and I.R. spectroscopies and element analysis before use. All chemicals used were analytical grade and the solvents were distilled before use. We notice also that R1 is an insoluble compound in acid solution. The molecular structure of Qx1 is shown in scheme 1.



Diam1: amino-2-aniline; **R1** : 1,6-dihydroxy-1,6-diphenylhexa-1,5-diene-3,4-dione; **Qx1:** 2-[3-(2-oxo-2-phenylethylidene)-1,4-dihydroquinoxaline-2(1H)-ylidene]-1-phenylethanone

Scheme 1. Molecular structure of the quinoxaline derivative.

Gravimetric, polarisation and impedance spectroscopy measurements

Prior to all measurements, the steel specimens (0.09 % P; 0.38 % Si; 0.01 % Al; 0.05 % Mn; 0.21 % C; 0.05 % S; Fe balance) were abraded with different emery paper up to 1000 grade, washed thoroughly with bidistilled water, degreased and dried with acetone. The aggressive solution (1 M HCl) was prepared by dilution of analytical grade 37% HCl with bidistilled water.

Gravimetric measurements were carried out in a double walled glass cell equipped with a thermostat-cooling condenser. The solution volume was 100 cm³. The steel specimens used had a rectangular form (2 cm x 2 cm x 0.05 cm).

Electrochemical measurements were carried out in a conventional three electrode electrolysis cylindrical pyrex glass cell. The working electrode (W.E.) had the form of a disc cut from the steel sheet. The area exposed to the corrosive solution was 1 cm². A saturated calomel electrode (SCE) and a disc platinum electrode were used respectively as reference and auxiliary electrodes. The temperature was thermostatically controlled at 308 ± 1 K.

Polarisation curves were recorded with a potentiostat (Amel 549) using a linear sweep generator (Amel 567) at a scan rate of 0.33 mV/s. Before recording the polarisation curves, the test solution was de-aerated and magnetically stirred for 30 min in the cell with nitrogen. The steel electrode, kept at its open circuit value, was polarised at -800 mV for 10 min. The potential of the electrode was then swept. Gas bubbling was maintained throughout the experiments.

Electrochemical impedance spectroscopy (EIS) was carried out with a Tacussel electrochemical system at E_{corr} after immersion in solution without bubbling, the circular surface of steel exposing of 1 cm² to the solution was used as working electrode. After the determination of steady-state current at a given potential, sine wave voltage (10 mV) peak to peak, at frequencies between 100 kHz and 10 mHz were superimposed on the rest potential. Computer programs automatically controlled the measurements performed at rest potentials after 30 min of exposure. The impedance diagrams are given in the Nyquist representation.

Results and discussion**Weight loss tests**

The effect of addition of quinoxaline and diamine compounds tested at different concentrations on the corrosion of steel in 1 M HCl solution was studied by weight-loss method at 308 K after 6 hours of immersion. Inhibition efficiency (E_w%) is calculated as follows (equation below):

$$E_w \% = \left(1 - \frac{W_{\text{corr}}}{W_{\text{corr}}^0} \right) 100 \quad (1)$$

where W_{corr} and W_{corr}⁰ are the corrosion rates of steel with and without organic compound, respectively.

Table 1 shows the results of weight loss of steel in 1 M HCl with and without the addition of various concentrations of Qx1 and Diam1. It is clear that the corrosion rate decreases with the concentration of the compounds tested. Qx1 shows a higher inhibitory power compared to Diam1. The inhibition efficiency, E%, attains 81% and 50% at 10⁻⁴ M, respectively.

The protective properties of Qx1 are probably due to the interaction between π -electrons of the three aromatic rings of the quinoxaline and the free pairs of electrons of N and O atoms with the positively charged steel surface.

Table 1. Effect of Qx1 and Diam1 concentration on corrosion of steel in 1 M HCl (308 K and 6 h).

	Concentration (M)	Corrosion rate $W(\text{mg.cm}^{-2}.\text{h}^{-1})$	Efficiency ($E_w\%$)
HCl	1	0.661	-
Qx1	10^{-4}	0.124	81
	5×10^{-5}	0.184	72
	10^{-5}	0.234	65
	5×10^{-6}	0.338	49
	10^{-6}	0.400	39
	10^{-7}	0.479	27
Diam1	10^{-3}	0.174	74
	5×10^{-4}	0.297	55
	10^{-4}	0.333	50
	5×10^{-5}	0.363	45
	10^{-5}	0.407	38
	10^{-6}	0.485	25

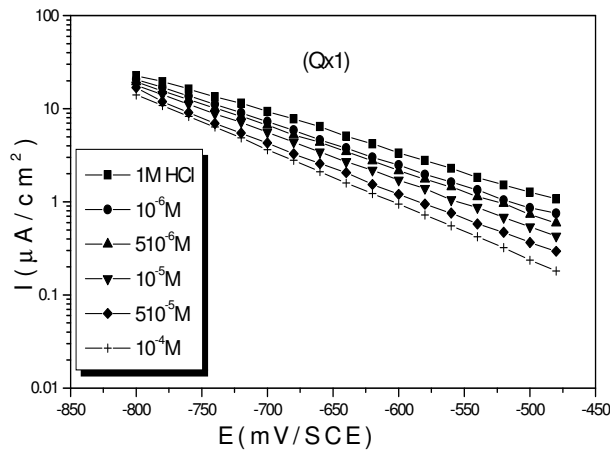


Figure 1. Polarisation curves of steel in 1 M HCl for various concentrations of Qx1.

Polarisation results

The influence of concentration of Qx1 and Diam1 on the cathodic polarisation curves of steel in 1 M HCl is studied at 298 K. Fig. 1 shows the typical curves obtained by Qx1 addition. Table 2 gives values of corrosion current (I_{corr}), corrosion potential (E_{corr}), and cathodic Tafel slope (b_c). In this case, the relation below (equation 2) determines the inhibition efficiency ($E_i\%$):

$$E_i\% = \left(1 - \frac{I_{\text{corr}}}{I_{\text{corr}}^0}\right) \cdot 100 \quad (2)$$

where I_{corr}^0 and I_{corr} are the uninhibited and inhibited corrosion current densities, respectively, determined by extrapolation of cathodic Tafel lines to corrosion potential.

Table 2. Electrochemical parameters of steel in 1 M HCl + Diam1 and Qx1 at various concentrations, and the corresponding inhibition efficiency.

	Concentration (M)	E_{corr} (mV/SCE)	b_c (mV/dec)	I_{corr} ($\mu\text{A}/\text{cm}^2$)	($E_i\%$)
HCl	1	-470	217	1000	-
Qx1	10^{-4}	-460	169	147	85
	5×10^{-5}	-465	179	232	77
	10^{-5}	-462	197	337	66
	5×10^{-6}	-460	211	504	50
	10^{-6}	-461	215	581	42
Diam1	10^{-3}	-458	200	238	76
	10^{-4}	-465	210	468	53
	5×10^{-5}	-467	206	518	48
	10^{-5}	-466	209	584	42
	10^{-6}	-461	215	662	34

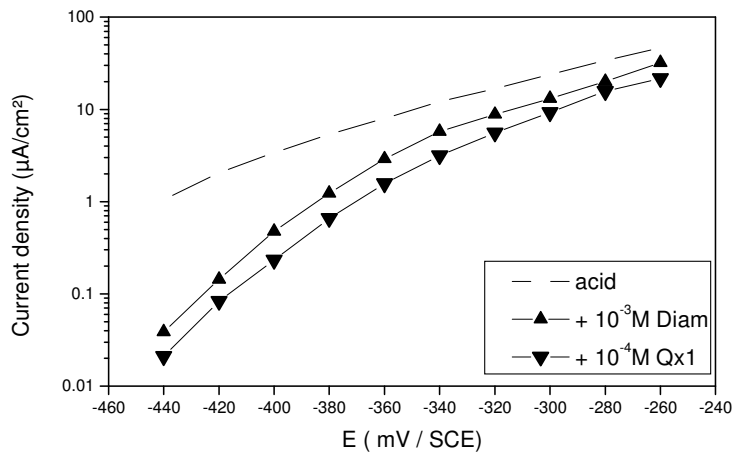


Figure 2. Polarisation curves of steel in 1 M HCl and added by 10^{-3} M Diam and 10^{-4} M Qx1.

As it is shown in Fig. 1 and Table 2, cathodic polarisation curves rise to parallel Tafel lines, indicating that the hydrogen evolution reaction is activation controlled. Thus, the presence of diamine and quinoxaline compounds does not affect the mechanism of this process. The addition of molecules tested causes a

decrease of the current density. The values of corrosion potential (E_{corr}) and cathodic Tafel slope (b_c) remain almost constant upon the addition of inhibitor concentration. The results demonstrate that the hydrogen reduction is inhibited and that the inhibition efficiency increases with inhibitor concentration to attain 85 % at 10^{-4} M and 76% at 10^{-3} M for Qx1 and Diam1, respectively.

The anodic curves obtained in Fig. 2 indicate that the inhibition mode of Diam1 and Qx1 does not depend upon electrode potential. The presence of Diam1 and Qx1 decreases the anodic current density versus potential characteristics. The anodic inhibitory action of Qx1 is better than that of Diam1. This result indicates that Qx1 and Diam1 act as mixed inhibitors.

Electrochemical impedance spectroscopy (EIS)

Electrochemical impedance spectroscopy (EIS) measurements have been carried out at 308 K in acidic solution with and without quinoxaline compound. The charge-transfer resistance (R_t) values were calculated from the difference in impedance at lower and higher frequencies. The double layer capacitance (C_{dl}) and the frequency at which the imaginary component of the impedance is maximal ($-Z_{\text{max}}$) were calculated from the equation (3) below:

$$C_{dl} = \left(\frac{1}{\omega R_t} \right) \tag{3}$$

where $\omega = 2\pi f_{\text{max}}$

The inhibition efficiency got from the charge transfer resistance is calculated by using equation (4):

$$E_z (\%) = 100 . (1 - R_t / R_{t/inh}) \tag{4}$$

where R_t and $R_{t/inh}$ are the charge transfer-resistance values with and without inhibitor, respectively.

Table 3. Impedance parameters for steel in 1 M HCl for various concentrations of Qx1.

	Concentration	R_t ($\Omega \cdot \text{cm}^2$)	f_{max} (Hz)	C_{dl} ($\mu\text{F}/\text{cm}^2$)	$E_z\%$
HCl 1 M	1 M	90	40	44.23	-
Qx1	10^{-6} M	145	25	43.92	40
	10^{-5} M	230	15.82	43.76	61
	10^{-4} M	510	10	31.22	82

The impedance parameters derived from these investigations at E_{corr} are presented in Table 3. As observed in Fig. 3, the impedance diagrams consist of one large capacitive loop. In fact, the presence of quinoxaline compounds enhances the value of R_t in acidic solution, indicating a charge transfer process mainly controlling the corrosion of steel. Values of double layer capacitance decrease to the maximum extent in the presence of Qx1. This result is due to the

adsorption of Qx1 on the metal surface leading to the formation of film from acidic solution [32].

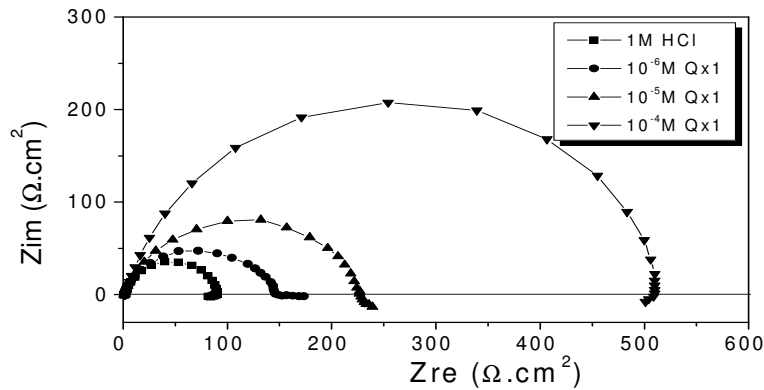


Figure 3. Nyquist plots of steel in 1M HCl containing various concentrations of Qx1 at E_{corr} .

In order to get more information about the action of Qx1 on the partial branches of corrosion behaviour of steel, EIS diagrams were recorded at cathodic (-600 mV) and anodic (-300 mV) potentials. Table 4 shows the corresponding EIS parameters. We observed a noticeable decrease of R_t in the anodic range due to the higher dissolution of steel in acid compared to those in cathodic and at E_{corr} . But, a greater increase of R_t is observed both in cathodic, E_{corr} , and anodic potentials in inhibited acid than in free acid. The efficiencies obtained are 77, 82 and 73% at -600 mV, E_{corr} and -300 mV, respectively. These results confirm that Qx1 adsorbs both on cathodic and anodic domains and therefore acts as a mixed type-inhibitor.

Table 4. EIS parameters obtained at cathodic (-600 mV), E_{corr} and anodic (-300 mV) potentials.

	R_t ($\Omega.cm^2$)	f_{max} (Hz)	C_{dl} ($\mu F/cm^2$)	Ez%
1 M HCl at -600 mV	33	158.2	30.50	-
+ 10^{-4} M Qx1 at -600 mV	141	25	45.17	77
1 M HCl at E_{corr}	90	40	44.23	-
+ 10^{-4} M Qx1 at E_{corr}	510	10	31.22	82
1 M HCl at -300 mV	5.2	100	306.2	-
+ 10^{-4} M Qx1 at -300 mV	20	250	31.7	73

Effect of temperature

The effect of temperature on the corrosion rate of steel in free acid and on addition of 10^{-4} M Qx1 at 1 hour immersion period from 308 to 353 K is shown in Table 5.

Table 5. Effect of temperature on the steel corrosion in free acid and on addition of 10^{-4} M of Qx1 at 1 h immersion period.

T (K)	1 M HCl	1 M HCl + 10^{-4} M Qx1	
	W^0 (mg.h ⁻¹ .cm ⁻²)	W (mg.h ⁻¹ .cm ⁻²)	$E_w\%$
308	0.661	0.124	81
313	0.858	0.215	75
323	1.437	0.572	60
333	2.725	1.506	45
343	5.388	3.981	26
353	10.649	7.978	25

It is clear that the corrosion rate increased considerably with the rise of temperature for blank solution. In the presence of the tested molecules, the corrosion rate is highly reduced at moderate temperatures. We observed that the efficiency depends on the temperature and decreases with temperature up to 25% at 353 K. This can be explained by the decrease of the strength of the adsorption processes at elevated temperature, suggesting a physical adsorption mode.

The logarithm of the corrosion rate of steel W_{corr} can be represented as a straight-line (Fig. 4) function of $1000/T$ (Arrhenius equation, equation 5), where T is the temperature in Kelvin:

$$W_{corr} = K \exp(-E_a/RT) \quad \text{and} \quad W^0_{corr} = K' \exp(-E'_a/RT) \quad (5)$$

$E'_a = 83.1$ and $E_a = 57.8$ kJ/mol are the activation energy with and without Qx1, respectively.

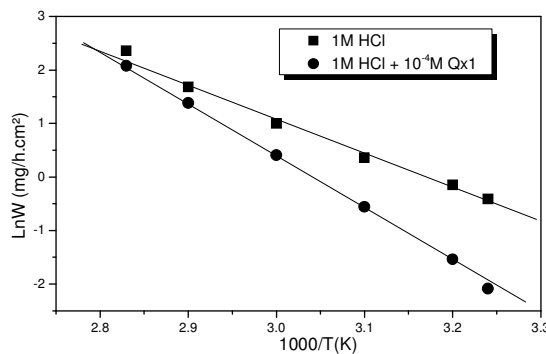


Figure 4. Arrhenius plots of steel in 1 M HCl in the absence and presence of 10^{-4} M Qx1.

It is observed that E_a increases in the presence of inhibitor, which indicates poor performance of Qx1 at higher temperatures. This increase of activation energy is generally interpreted as an electrostatic adsorption process of inhibitor on the steel surface [33,34].

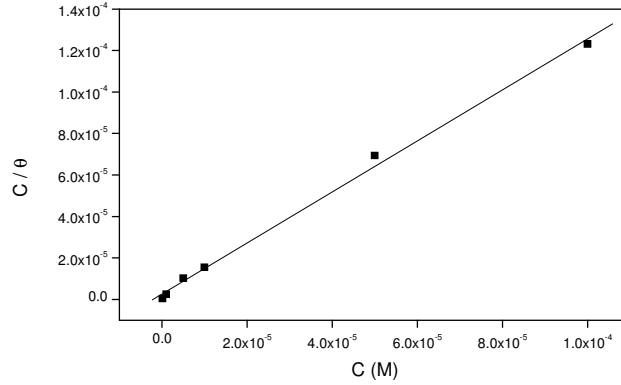


Figure 5. Langmuir isotherm adsorption of quinoxaline on steel in 1 M HCl.

Adsorption isotherm

Fig. 5 illustrates the dependence of the fraction of the concentration and the effective surface covered C/θ as a function of the concentration of the quinoxalines. θ is the ratio $E / 100$. The obtained plot is linear with a slope equal to 1.23 near to unity, showing an adsorption on the steel surface electrode according to the Langmuir [35] isotherm (equation 6):

$$\frac{C}{\theta} = C + \frac{1}{K} \tag{6}$$

with $K = \frac{1}{55.55} \exp\left(-\frac{\Delta G_{ads}^0}{RT}\right)$. K is the equilibrium constant leading to the standard free energy of adsorption, ΔG_{ads} .

The values obtained for the equilibrium constant K and ΔG_{ads}^0 are 354862 and -43.04 kJ/mol, respectively. The negative value of ΔG_{ads}^0 indicates that Qx1 is strongly adsorbed on the steel surface [36]. The nature of the adsorption process can be clarified further if the heat of adsorption ΔH_{ads}^0 value is known. It has been shown [37] that for $\Delta H_{ads}^0 < 10$ kJ/mol the adsorption is most probably physical in character, while for $\Delta H_{ads}^0 > 10$ kJ/mol chemisorption is expected. The determination of ΔH_{ads}^0 may be deduced from the Langmuir adsorption expression below (equation 7) [35]:

$$\ln \frac{\theta}{1 - \theta} = \ln A + \ln C - \frac{\Delta H_{ads}^0}{RT} \tag{7}$$

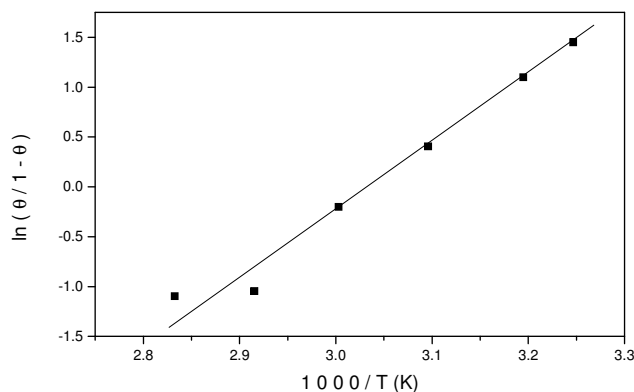


Figure 6. Heat of adsorption determination from the plot of $\ln(\theta/1-\theta)$ vs. $1000/T$ for 10^{-4} M Qx1.

The slope of the straight line obtained in Fig. 6 equals to $-\Delta H_{\text{ads}}^{\circ}/R$. The heat of adsorption obtained is -54.86 kJ/mol. The negative value obtained shows that the adsorption is an exothermic phenomenon. Also, the relatively low $\Delta H_{\text{ads}}^{\circ}$ verifies the physical adsorption character of the adsorption. The adsorption entropy $\Delta S_{\text{ads}}^{\circ}$ deduced is -39.7 J/mol. The negative value of ΔS° means that the adsorption process is accompanied by a decrease in entropy and a disordered layer of Qx1 molecules takes place on the steel surface. The inhibitory action of Qx1 may be explained by an intramolecular synergistic effect between secondary diamine and the rest of molecule.

Conclusion

- The quinoxaline studied Qx1 and Diam 1 are good inhibitors for steel in 1 M HCl.
- The inhibition efficiency of Qx1 increases with the increase of the concentration up to 85% at 10^{-4} M.
- Qx1 and Diam1 act as mixed-type inhibitors without modifying the mechanism of hydrogen evolution.
- The inhibition efficiency of Qx1 decreases with increase in temperature.
- Qx1 adsorbs on the steel surface according to the Langmuir adsorption isotherm.

References

1. H. Shokry, M. Yuasa, I. Sekine, R.M. Issa, H.Y. El-baradie, G.K. Gomma, *Corros. Sci.* 40 (1998) 2173. 10.1016/S0010-938X(98)00102-4
2. Sk.A. Ali, M.T. Saeed, *Polymer* 42 (2001) 2785. 10.1016/S0032-3861(00)00665-0
3. A. Ouchrif, M. Zegmout, B. Hammouti, A. Dafali, M. Benkaddour, A. Ramdani, S. Elkadiri, *Prog. Org. Coat.* 53 (2005) 292. 10.1016/j.porgcoat.2005.02.010

4. M. Bouklah, B. Hammouti, A. Aouniti, M. Benkaddour, A. Bouyanzer, *Appl. Surf. Sci.* 252 (2006) 6236. 10.1016/j.apsusc.2005.08.026
5. B. Hammouti, A. Aouniti, M. Taleb, M. Brighli, S. Kertit, *Corrosion* 51 (1995) 411.
6. R. Salghi, B. Hammouti, S. Kertit, *Bull. Electrochem.* 13 (1997) 399.
7. M. Zerfaoui, H. Oudda, B. Hammouti, M. Benkaddour, S. Kertit, M. Zertoubi, M. Azzi, M. Taleb, *Revue de métallurgie* 99 (2002) 1105. 10.1051/metal:2002156
8. D. Bouzidi, S. Kertit, B. Hammouti, M. Brighli, *J. Electrochem. Soc. India* 46 (1997) 23.
9. R. Salghi, B. Hammouti, A. Aouniti, M. Berrabah, S. Kertit, *J. Electrochem. Soc. India* 49 (2000) 40.
10. R. Salghi, L. Bazzi, E. Ait Addi, B. Hammouti, *Transactions of the SAEST* 38 (2003) 127.
11. M. Zerfaoui, B. Hammouti, H. Oudda, M. Benkaddour, *Prog. Org. Coat.* 51 (2004) 134. 10.1016/j.porgcoat.2004.05.005
12. F. Touhami, A. Aouniti, S. Kertit, Y. Abed, B. Hammouti, A. Ramdani, K. El-Kacemi, *Corros. Sci.* 42 (2000) 929. 10.1016/S0010-938X(99)00123-7
13. A. Chetouani, M. Daoudi, B. Hammouti, T. Ben Hadda, M. Benkaddour, *Corros. Sci.* 48 (2006) 2987. 10.1016/j.corsci.2005.10.011
14. K. Tebbji, I. Bouabdellah, A. Aouniti, B. Hammouti, H. Oudda, M. Benkaddour, A. Ramdani, *Mater. Lett.* 61 (2007) 799. 10.1016/j.matlet.2006.05.063
15. L. Herrag, A. Chetouani, S. Elkadiri, B. Hammouti, A. Aouniti, *Port. Electrochim. Acta* 26 (2008) 211. 10.4152/pea.200802211
16. K. Laarej, M. Bouachrine, S. Radi, S. Kertit, B. Hammouti, *E-Journal of Chemistry* 7 (2010) 419.
17. R. Salghi, L. Bazzi, B. Hammouti, E. Zine, S. Kertit, S. El Issami, E. Ait Eddi, *Bull. Electrochem.* 17 (2001) 429.
18. B. Zerga, A. Attayibat, M. Sfaira, M. Taleb, B. Hammouti, M. Ebn Touhami, S. Radi, Z. Rais, *J. Appl. Electrochem.* 40 (2010) 1575. 10.1007/s10800-010-0164-0
19. Y. Abed, B. Hammouti, S. Kertit, K. El Kacemi, A. Mansri, *Bull. Electrochem.* 17 (2001) 105.
20. O. Krim, A. Elidrissi, B. Hammouti, A. Ouslim, M. Benkaddour, *Chem. Eng. Comm.* 196 (2009) 1536. 10.1080/00986440903155451
21. A. Chetouani, K. Medjahed, K.E. Benabadji, B. Hammouti, S. Kertit, A. Mansri, *Prog. Org. Coat.* 46 (2003) 312. 10.1016/S0300-9440(03)00019-5
22. A. Chetouani, K. Medjahed, K.E. Sid-Lakhdar, B. Hammouti, M. Benkaddour, A. Mansri, *Corros. Sci.* 46 (2004) 2421. 10.1016/j.corsci.2004.01.020
23. M. Bouklah, A. Attayibat, B. Hammouti, A. Ramdani, S. Radi, M. Benkaddour, *Appl. Surf. Sci.* 240 (2004) 341. 10.1016/j.apsusc.2004.07.001
24. M. Benabdellah, R. Touzani, A. Aouniti, A. Dafali, S. Elkadiri, B. Hammouti, M. Benkaddour, *Phys. Chem. News* 37 (2007) 63.
25. M. Benabdellah, K. Tebbji, B. Hammouti, R. Touzani, A. Aouniti, A. Dafali, S. El Kadiri, *Phys. Chem. News* 43 (2008) 115.

26. A. Zarrouk, A. Dafali, B. Hammouti, H. Zarrok, S. Boukhris, M. Zertoubi, *Int. J. Electrochem. Sci.* 5 (2010) 46.
27. I. El Ouali, B. Hammouti, A. Aouniti, Y. Ramli, M. Azougagh, E.M. Essassi, M. Bouachrine, *J. Mater. Environ. Sci.* 1 (2010) 1.
28. H. Gali-Muhtasib, M. Sidani, F. Geara, A-D. Mona, J. Al-Hmaira, M.J. Haddadin, G. Zaatari, *Int. J. Oncol.* 24 (2004) 1121.
29. S. Piras, M. Loriga, G. Paglietti, *Il Farmaco* 59 (2004) 185. 10.1016/j.farmac.2003.11.014
30. A. Jaso, B. Zarranz, I. Aldana, A. Monge, *Tubérculos* 38 (2003) 791.
31. A. Carta, M. Loriga, G. Paglietti, A. Mattana, P.L. Fiori, P. Mollicotti, L. Sechi, S. Zanetti, *Eur. J. Med. Chem.* 39 (2004) 195. 10.1016/j.ejmech.2003.11.008
32. F. Bentiss, M. Lagrenée, M. Traisnel, J.C. Hornez, *Corros. Sci.* 41 (1999) 789. 10.1016/S0010-938X(98)00153-X
33. A. Popova, E. Sokolova, S. Raicheva, M. Christov, *Corros. Sci.* 45 (2003) 33. 10.1016/S0010-938X(02)00072-0
34. T. Szauer, A. Brandt, *Electrochim. Acta* 26 (1981) 1209. 10.1016/0013-4686(81)85101-8
35. I. Langmuir, *J. Am. Chem. Soc.* 39 (1947) 1848. 10.1021/ja02254a006
36. Y.A. El-Awady, A.I. Ahmed, *J. Ind. Chem.* 24A (1985) 601.
37. A.E. Stoyanova, E.I. Sokolova, S.N. Raicheva, *Corros. Sci.* 39 (1997) 1595. 10.1016/S0010-938X(97)00063-2